

Effect of Tool Shoulder Diameter on Stir Zone Characteristics of Friction Stir Welded HSLA Steel Joints

S. Ragu Nathan¹  · V. Balasubramanian² · S. Malarvizhi² · A. G. Rao³

Received: 16 August 2015 / Accepted: 31 January 2016 / Published online: 25 March 2016
© The Indian Institute of Metals - IIM 2016

Abstract In this study, the effect of tool shoulder diameter (primary heat generating source) to the plate thickness ratio on tensile and impact toughness properties of friction stir welded high strength low alloy (HSLA) steel was investigated. A naval grade HSLA steel of 5 mm thick plates were welded with tool rotational speed of 600 rpm and welding speed of 30 mm/min using five tungsten based alloy tools having shoulder diameter varying from 20 to 30 mm. Microstructural characteristics of the weld joints were analyzed using optical microscopy along with the evaluation of tensile properties. From this investigation, it was found that the joint fabricated using a tool shoulder diameter of 25 mm (5 times the plate thickness) exhibited superior mechanical properties compared to other joints.

Keywords Friction stir welding · HSLA steel · Tensile properties · Impact toughness · Microstructure

1 Introduction

High strength low alloy (HSLA) steels have been primarily developed to replace low-carbon steels for the automotive industry in order to improve the strength-to-weight ratio and meet the need for higher-strength construction grade materials. HSLA steels demonstrate unique properties such as high strength, excellent ductility, and good weldability, and also exhibit outstanding low temperature impact toughness superior to that of high yield strength (HY) steels. HSLA steels have much improved weldability compared to HY steels [1]. Now-a-days, the micro-alloyed or HSLA steels become an indispensable class for different applications like construction of large ships, oil and gas transmission lines, offshore oil drilling platforms, pressure vessels, building construction, bridges, storage tanks.

Fusion welding of these grade of steels, generally encounter hydrogen induced cracking at the heat affected zone (HAZ) and the only way to weld such steels is to use low hydrogen ferritic steel filler wire [2]. Charpy impact toughness of HSLA steel has been improved by inter-critical heat treatment which enhances the microstructure through the formation of ferrite microstructure with various morphologies, irregular martensite and 75 % of microstructure with high angle grain boundaries [3]. The resistance to hydrogen-induced cracking and stress corrosion cracking has been improved by coarse grain heat affected zone which consists of martensite–austenite constituents, and thus showing the importance of reduction in carbon content of these steels [4].

Friction stir welding (FSW) is a novel solid state joining technique that is presently attracting significant attention on welding of hard metals such as steel and titanium [5–7]. FSW has appeared as an easy, ecological and promising productive welding method that reduces material waste and avoids radiation and harmful gas emissions, usually associated with the

✉ S. Ragu Nathan
ragucemajor@gmail.com

V. Balasubramanian
visvabalu@yahoo.com

S. Malarvizhi
jeejoo@rediffmail.com

A. G. Rao
gouravdrdo@gmail.com

¹ Department of Manufacturing Engineering, Annamalai University, Annamalai Nagar, Tamil Nadu 608 002, India

² Centre for Materials Joining & Research (CEMAJOR), Department of Manufacturing Engineering, Annamalai University, Annamalai Nagar, Tamil Nadu 608 002, India

³ Marine Materials Division, Naval Materials Research Laboratory (NMRL), Ambernath, Mumbai, Maharashtra 421 506, India

fusion welding processes. Mechanical action in the form of frictional stirring on the base material has modified the microstructure from coarse grains to very fine grains due to plastic deformation and fast cooling rate [8–10]. Welding of steel is affected by both the temperature and composition which extensively affects the microstructure evolution. Friction stir welding enables to control these factors and produce superior joint strength [1]. Much of the tool degradation may be attributed to the high heat (temperature around 1200 °C) and the stresses generated during friction stir welding of these high strength materials. However, the development of the wear resistant tool materials has benefited the FSW process and paved way for the rapid implementation of this process in the fabrication of high strength steel structures [11, 12].

Though the tool has different portions (pin, shoulder and shank), shoulder diameter and pin diameter controls the frictional heat generation during welding. Of the two, shoulder diameter is the predominant heat generating source since the contact area between shoulder and surface of the base metal is higher than the other contact areas [10]. Hence, in this investigation, an attempt has been made to study the effect of tool shoulder diameter on microstructural characteristics and mechanical properties of friction stir welded HSLA steel joints.

2 Experimental

The rolled plates of naval grade HSLA steel with thickness of 5 mm were cut to the required dimensions (150 mm × 300 mm) by abrasive cutting to prepare the

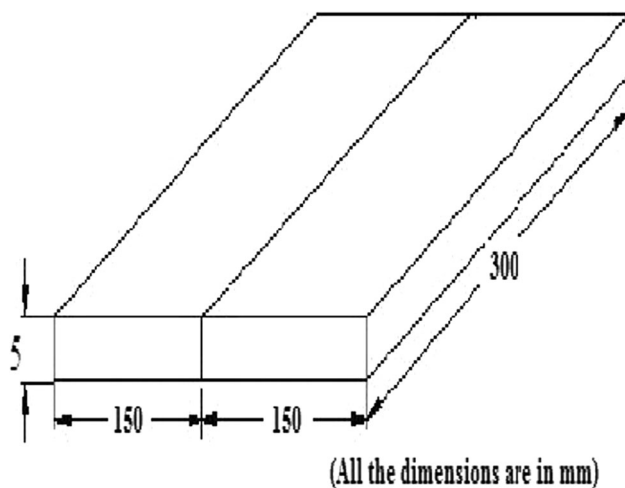


Fig. 1 Joint configuration for FSW

Table 1 Chemical composition (wt%) of parent metal

C	Mn	N	Si	Mo	Ti	V	Nb	Ni	Cu	Al	W
0.08	1.42	0.015	0.19	0.02	0.016	0.032	0.035	0.69	0.126	0.032	0.04

joint configurations as shown in Fig. 1. The chemical composition of parent metal is presented in Table 1. The microstructure of parent metal is displayed in Fig. 2. It is composed of ferrite with small amount of pearlite. Non-consumable tools made of tungsten base alloy were used to weld the joints using FSW process. The tools were manufactured through powder metallurgy route having various shoulder diameter of 20, 22.5, 25, 27.5 and 30 mm and a tapered pin, tapering from 12 mm at the shoulder to 8 mm at the pin tip (Fig. 3). Welding parameters used to fabricate the joints are presented in Table 2. Indigenously designed and developed computer numeric controlled FSW machine (6.0 kN capacity) was used to weld the HSLA steel plates. The welding setup is shown in Fig. 4.

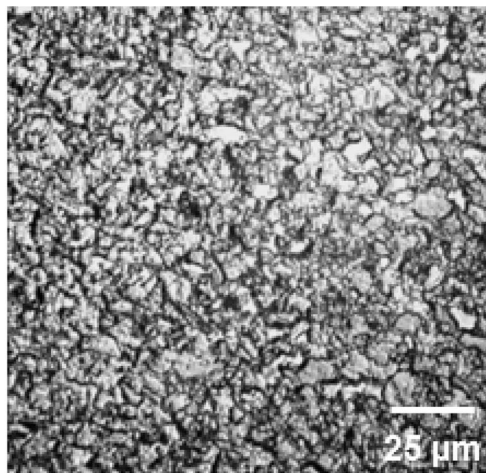
ASTM E8 M-04 guidelines were followed for preparing the tensile test specimens. Electromechanical controlled universal testing machine (100 kN capacity) was used to evaluate the tensile properties. Charpy impact specimens were prepared to evaluate the impact toughness of the weld metal and hence the notch was placed (machined) in the weld metal (weld center). Since the plate thickness was small, sub size specimens were prepared. Impact testing was conducted on a pendulum-type impact testing machine (300 J capacity) at room temperature. The amount of energy absorbed in fracture was recorded. The absorbed energy is defined as the impact toughness of the joint.

Vickers's microhardness tester was used for measuring the hardness distribution across the welded joint along the mid thickness region with a load of 0.5 N. The specimen for metallographic examination was sectioned to the required size from the joint comprising weld metal, HAZ (heat-affected zone), and base metal regions, and polished using different grades of emery papers. Final polishing was done using the diamond compound (particle size of 1 μm) on the disc polishing machine. Specimens were etched with 2 % of Nital solution to reveal the microstructural features of the joints. Microstructural examination was carried out using an optical microscope incorporated with an image analyzing software (Metal Vision).

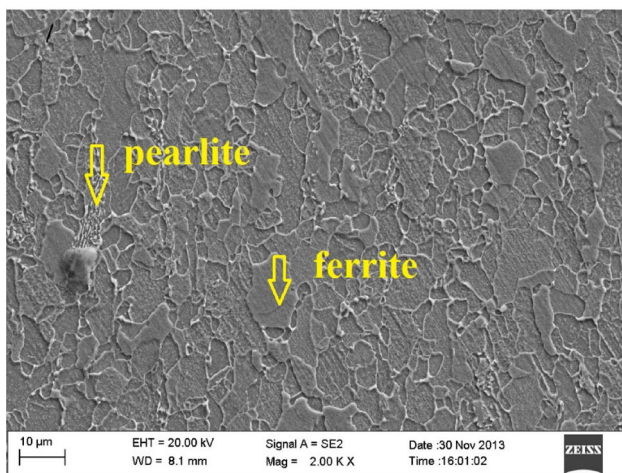
3 Results

3.1 Cross-Sectional Macrographs

The cross-sectional macrographs of the welded joints are presented in Table 3. The cross-section of FSW joint appears like 'basin-shape'. It comprises of advancing side heat



(a)



(b)

Fig. 2 Micrographs of parent metal. **a** Optical micrograph, **b** SEM micrograph

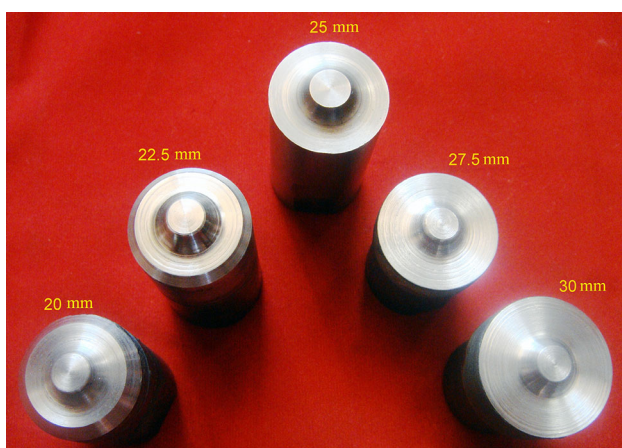


Fig. 3 Photograph of FSW Tools

Table 2 FSW conditions and welding parameters

Process parameters	Values
Rotational speed (rpm)	600
Welding speed (mm/min)	30
D/Tp ratio of tool	4, 4.5, 5, 5.5, and 6
Tool shoulder diameter (mm)	20, 22.5, 25, 27.5, and 30
Pin length (mm)	4
Tool inclined angle (°)	0

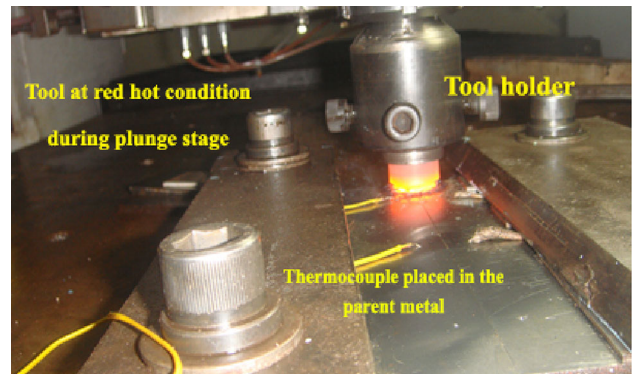


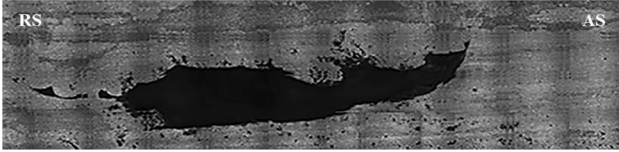

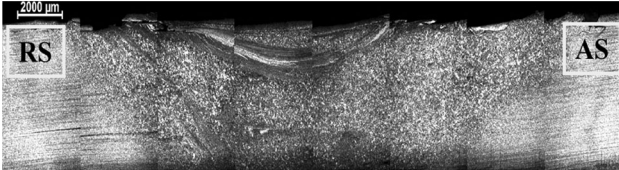

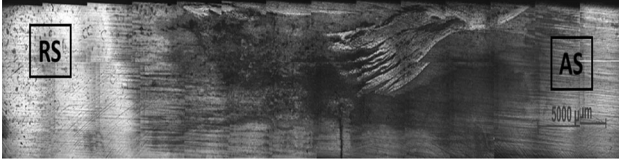
Fig. 4 FSW experimental setup

affected zone (ASHAZ), advancing side thermo-mechanically affected zone (ASTMAZ), stir zone (SZ), retreating side thermo-mechanically affected zone (RSTMAZ), retreating side heat affected zone (RSHAZ), weld metal (SZ) and heat affected zone (HAZ). The joint that is fabricated using a tool with the shoulder diameter of 25 mm (5 time plate thickness) yields defect free sound joint. Similarly, the joint that is fabricated using tool with the shoulder diameter of 20 mm (4 time plate thickness) yields tunnel defect at the advancing side of the joint, whereas the joint that has been fabricated using a tool with the shoulder diameter of 22.5 mm (4.5 time plate thickness) suffers incomplete welding due to lack of stirring. The other two joints, which are fabricated using tool with the shoulder diameter of 27.5 and 30 mm respectively results with pinhole defect, kissing bond and excess flash formation.

3.2 Microstructure

The cross section of the defect free joint has been analyzed using optical microscopy. Figure 5a–f represent the microstructure of different locations of defect free joint fabricated using a tool with 25 mm of shoulder diameter. Figure 5a shows the microstructure in the RSTMAZ (shoulder influenced region). Formation of band structure in the stir zone is clearly seen in the Fig. 5b. It clearly

Table 3 Influence of tool shoulder on macrostructure

D/Tp ratio	Macrostructure	Observations
4 (20 mm)		Tunnel defect at advancing side (0.848 kJ/mm)
4.5 (22.5 mm)		Lack of stirring at the bottom side of the plates (swirl zone) (0.954 kJ/mm)
5 (25 mm)		No defect (1.05 kJ/mm)
5.5 (27.5 mm)		Kissing bond at swirl zone, pin hole at advancing side (1.166 kJ/mm)
6 (30 mm)		Excess flash formation (1.272 kJ/mm)

shows that the high frictional heat has been generated in the shoulder influenced region. The ASTMAZ microstructure presented in Fig. 5c reveals the sudden change in grain orientation due to the metal excavation from this zone to deposit in the retreating side (Fig. 5d). However, the pin influenced region shows the presence of fine ferrite laths dispersed in bainitic matrix (Fig. 5e, f).

Figure 6 presents the SEM micrographs of the welded joint using 25 mm tool shoulder diameter at high

magnifications. Figure 6a represents the shoulder influenced region microstructure and the severe deformation of the material is clearly evident from the figure. The coupled effect of thermal and mechanical forces are responsible for the grain orientation, thereby resulting in severe plastic deformation and more frictional stirring occurs in the pin influenced region (Fig. 6b, c). Formation of band microstructure (Fig. 6c) illustrates the generated mechanical forces at high temperatures during FSW process on

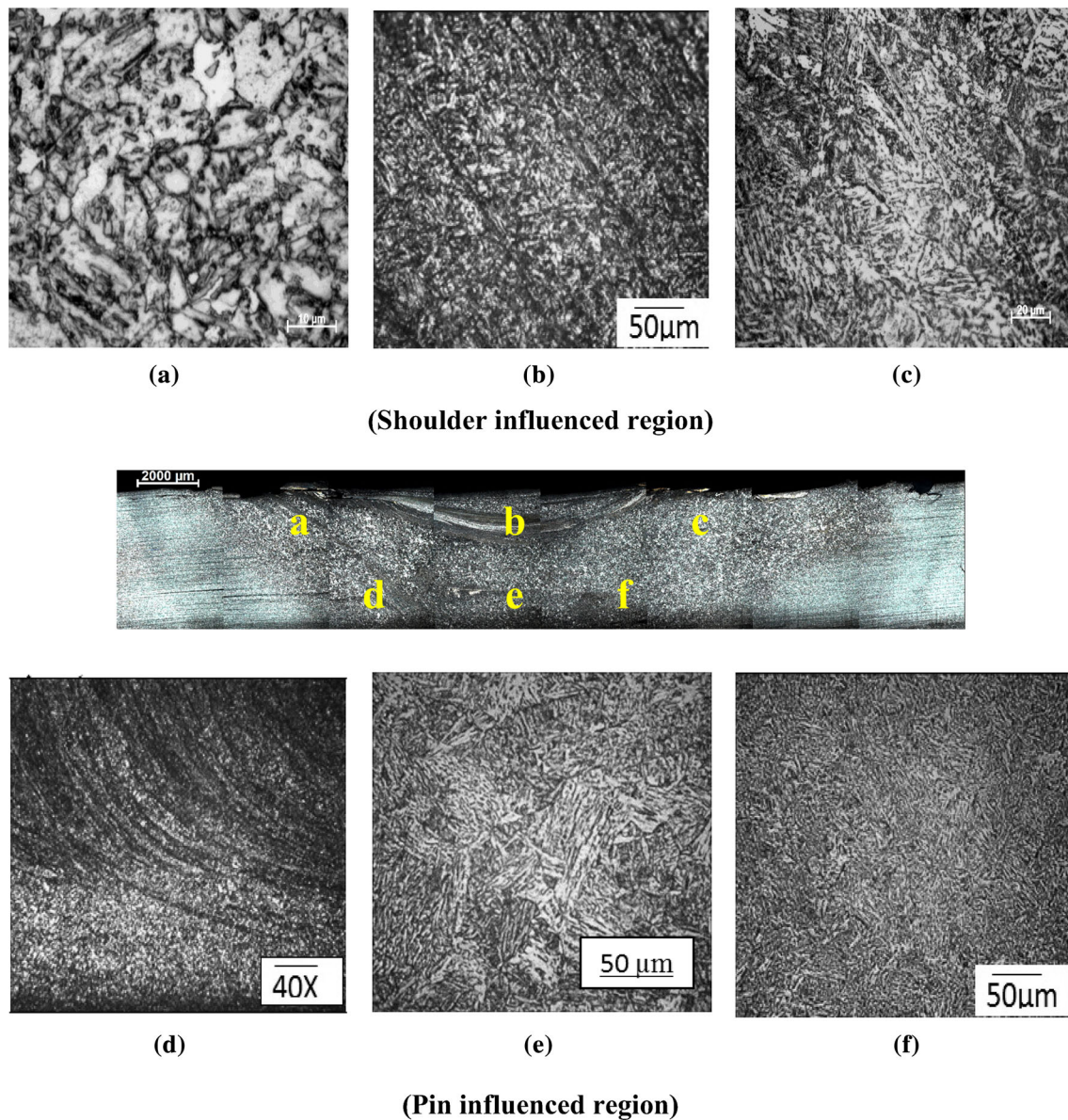


Fig. 5 Optical micrographs of various regions of welded steel joints. **a** RSTMAZ, **b** SZ, **c** ASTMAZ, **d** RSTMAZ, **e** SZ, **f** Swirl zone

HSLA steel plates. Hence, upper bainitic structure with fine lath ferrite microstructure in the stir zone of the weld joint fabricated using 25 mm shoulder diameter has been taken for further investigation on mechanical properties.

3.3 Tensile and impact toughness properties

The tensile properties of the parent metal and welded joints are presented in Table 4. The yield strength and tensile strength of parent metal is 438 and 610 MPa, respectively. But the yield strength and tensile strength of FSW joint are 502 and 664 MPa, respectively. The joints

that are fabricated using shoulder diameter to the plate thickness ratio of 5 (25 mm) by FSW process exhibits overmatched strength values and ductility values compared to parent metal.

Charpy impact toughness test results are presented in Table 4. The impact toughness of parent metal is 78 J at room temperature. When the weld metal is welded by FSW process, it exhibits 48 J, which is 38 % lower than that of the parent metal. The lowest impact strength is shown by the joint fabricated by FSW process compared to parent metal. FSW joint shows higher yield and tensile strength, lower elongation and toughness.

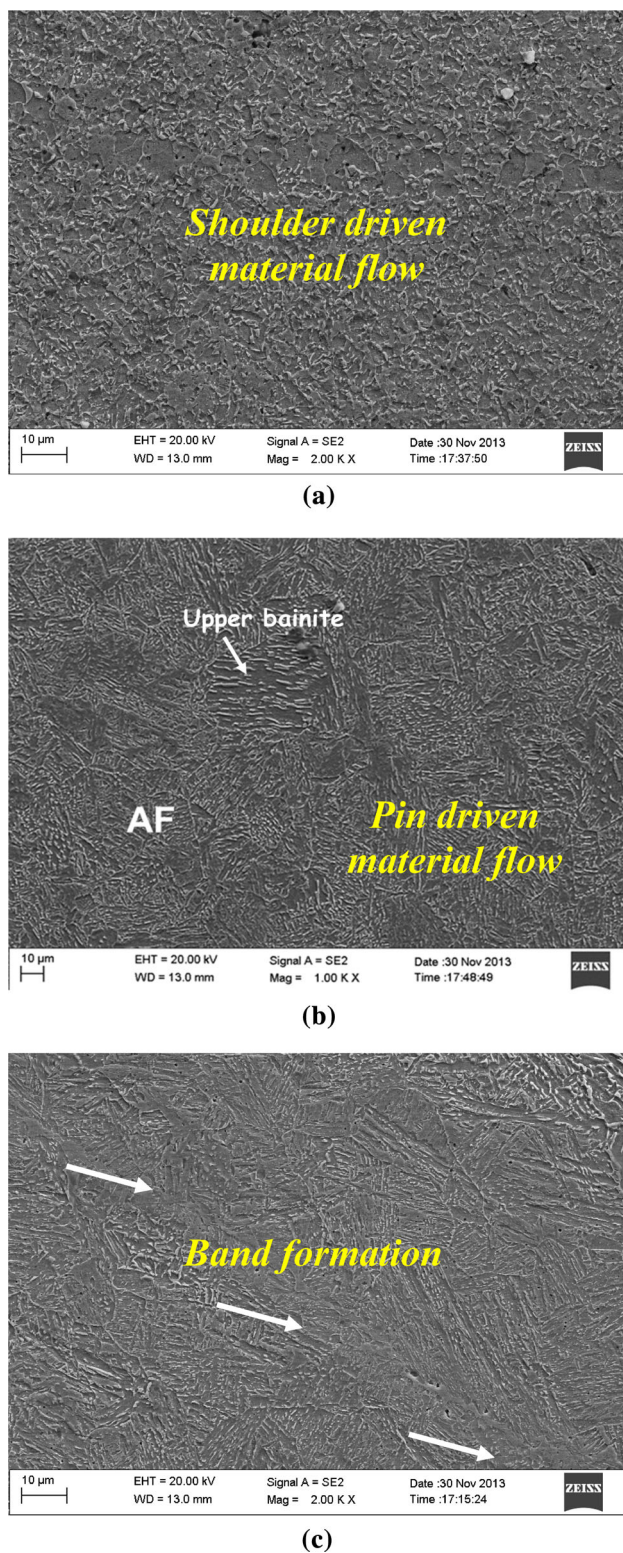


Fig. 6 SEM micrographs of weld region. **a** SZ (Shoulder influenced region), **b** SZ (middle), **c** SZ (Pin influenced region)

3.4 Microhardness

Figure 7 shows the hardness variations across the weld. The hardness of the as-received parent metal is approximately 270 HV. The hardness of stir zone varies from 300 to 410 HV, depending on the grain size and phases sampled from each indentation. The failure location of the welded joint is consistent with hardness distribution profile. The failure occurs in the joint along the lowest hardness distribution region (LHDR) [13].

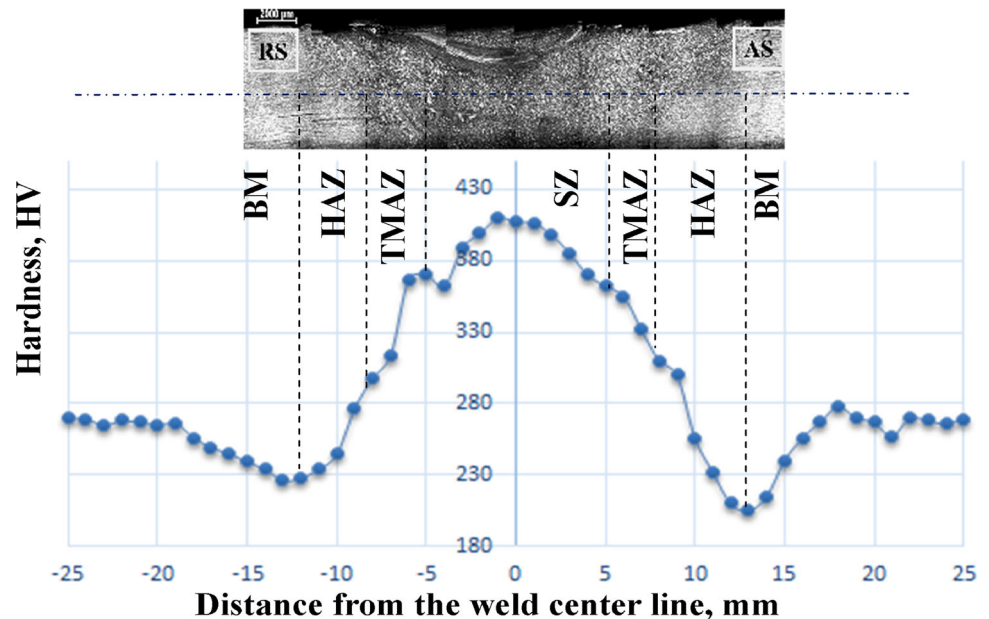
4 Discussion

In the case of FSW, the material is severely plastically deformed due to the stirring action of the pin tool, resulting in a fine grain structure. Dynamic recrystallization is a phenomena occurring during the material movement in FSW. The favorable material flow around the tool pin can be catered by suitable tool design selected particularly by considering the base metal properties. It may influence the tool life, weld quality and cost of the tool material too. Ability of the tool geometry in FSW process is to lead the material to root of the weld and to plasticize the material under the tool without change in dimension/configuration in the tool profile. The internal defects formation in the weld such as voids, increase in HAZ and root defects, mentioned in the Table 4 and shown in the Fig. 4, can be attributed to insufficient and inadequate material flow around the tool. In fact, as pointed out by Thompson and Babu [6], tool degradation in FSW of hard metals are influenced by flow stresses and welding temperatures that are generated during frictional stirring. The local stress is generated by increase in sticking torque which can increase the stress concentration at the corners of the tool pin and hence failure occurs. At the same time, due to compression of vertical force and resultant forces from the base metal are likely to reduce the densification of the matrix and crack propagates through the matrix phase of tool material.

The weld metal microstructure of welded joint is greatly influenced by the chemical composition and the heat input of the process. In general, higher heat input leads to slower cooling rate which results in the coarse grains in weld metal [14]. However, lower heat input leads to fast cooling rate which results in fine microstructure. Though the lower heat input can produce finer grains compared to higher heat input, the intrinsic nature of the process also plays major role in refining the weld metal microstructure. FSW process on HSLA steel using shoulder diameter of 25 mm

Table 4 Mechanical properties of the parent metal and defect free FSW joint

Joint	0.2 % offset yield strength (MPa)	Tensile strength (MPa)	Elongation in 25 mm gauge length (%)	Impact toughness @ RT (J)	Hardness of weld metal @ 0.5 N load (HV)	Fracture location
PM	438	610	29	78	270	Center
FSW	502	664	19	48	410	ASHAZ

Fig. 7 Microhardness survey across the cross-section of the welded joints. *LHDR* lowest hardness distribution region

supplies lower heat input (1.05 kJ/mm) to the weld region compared to other shoulder diameters (27.5 and 30 mm) which supply 1.166 and 1.272 kJ/mm, respectively. While the fast cooling rate (i.e., lower heat input) and mechanical action for refining microstructure process are coupled, formation of upper bainite with small amount of acicular ferrite is possible. This can be one of the reasons that FSW joint consists of upper bainite grains in the stir zone (Figs. 5b, 6b). Due to low heat generation in the SZ, RSTMAZ and ASTMAZ (Fig. 5a, c) the characteristics are also better. This may be due to unique weld metal characteristics and similar thermal properties of SZ, TMAZ, HAZ and PM [15]. An acicular ferrite microstructure has the potential of combining high strength and high toughness [16]. Microstructural stability is more in acicular ferrite compared to bainite in higher temperatures [17].

The post weld microstructure of the SZ consists of shear transformed bainitic ferrite with carbides and acicular ferrite, which can be the reason for higher hardness values (Fig. 7). The micro hardness values are less significant in affecting the mechanical properties, because the inherent nature of the tool rotational speed has more influencing factors over the hardness values [13]. Due to severe plastic deformation and mechanical stirring, the average grain size

of parent metal (15–19 μm approximately) has been refined to 3–5 μm in the stir zone as seen in Fig. 5e. This grain refinement mechanism was explained by Song et al. [25] as, the stored energy in the material is accompanied by severe deformation process that leads to increase in dislocation density. Due to this drastic grain refinement, the misorientation angle distributions are also altered in the stir zone. The stir zone is comparatively stronger, and the joint properties are controlled by weld metal chemical composition and microstructure. The strong carbide/nitride forming elements, like Nb, Ti, V, etc., have very limited solubility in ferrite and austenite, and normally the precipitates act as fine dispersion of carbides, nitrides and/or carbonitriding and contribute to strength due to precipitation hardening [18]. This may be the reason that the yield strengths of the joint increases compared to yield strength of the parent metal. The yield point elongation is attributed to the interaction of solute atoms and moving dislocations [19, 20].

The Table 4 clearly indicates that the strength of the FSW specimen is 8 % more than that of parent metal [21]. The increased strength is attributed to the fine grain microstructure consisting of acicular bainite, upper bainite and small cluster of martensite regions. Although the formation of martensite increases the strength, it decreases the

ductility and toughness. Also, the elongated spherical inclusions of MnS may also be an important factor in reducing the ductility. High angle grain boundaries ($>10^\circ$) result in enhancement of strength [12]. This is because, the plates of acicular ferrite nucleate intragranularly on non-metallic inclusions within large austenite grains, and then radiate in many different orientations from those inclusions whilst maintaining an orientation relationship with the austenite [22–24]. However, the misorientation angle between the grains can be the key feature in increasing the yield strength and tensile strength compared to parent metal.

Charpy V-notch impact toughness of parent metal is 78 J at room temperature, whereas the impact toughness of FSW joint exhibits 48 J which is 38 % lower than that of parent metal. The increased percentage of bainite leads to an enhancement of tensile properties, and the presence of small cluster of martensite is detrimental to impact toughness [22]. The presence of precipitate carbides raises the impact transition temperature and lowers the charpy shelf energy. The impact strength of upper bainite is adversely affected by the presence of cementite as thin film at the lath boundaries of bainite, increases the presence of martensite which does not contribute to strength but lowers the toughness [23, 24]. This may be the reason for reduction in toughness of FSW joint with respect to parent metal.

In FSW joint, the stir zone is exposed to maximum temperature with high strain rate. Subsequent fast cooling rate leads to the formation of upper bainite and lath bainitic microstructure in the stir zone. These two microstructures are the major contributors of the hardest stir zone in the FSW joint. Whereas in the HAZ and parent metal interface region, due to absence of dynamic recrystallization, low temperature exposure leads to formation of heterogeneous microstructure which consists of low angle grain boundaries with coarse grain structure. This may be the reason for low hardness distribution in the HAZ and base metal interface region [18, 25].

The tool shoulder diameter has a direct proportional relationship with the heat generation due to frictional stirring [13]. If the shoulder diameter is large, then heat generation due to friction will be high due to large contact area and vice versa. In this investigation it has been observed that the lower tool shoulder diameter (<25 mm) has less contact area and frictional force which leads to insufficient heat generation (0.848 kJ/mm). Thus the formation of defects are observed in the stir zone due to improper material flow because of inadequate plasticization of the parent metal in the stir zone. It has also been observed that the larger tool shoulder diameter (>25 mm) leads to wider contact area and results in more frictional heat generation (1.272 kJ/mm) and hence the turbulent flow of the plasticized material leads to excess weld flash

formation. On the other hand, higher grain refinement has been observed in the welds produced with the tool having shoulder diameter of 25 mm ($D/T_p = 5$) due to optimum heat generation (1.05 kJ/mm). The higher material is dragged and proper consolidation of that dragged material at the advancing side without any interface gap has been achieved in this 25 mm shoulder diameter. Therefore, as compared with other tool shoulder diameters, 25 mm shoulder diameter has better stability at elevated temperature and can be used for FSW of HSLA steel of 5 mm thickness.

5 Conclusions

In this investigation, an attempt was made to study the effect of tool shoulder diameter on stir zone characteristics of friction stir welded HSLA steel joints. From this investigation, the following important conclusions have been derived.

1. Of the five welded joints, the joint fabricated using a tool with the shoulder diameter of 25 mm (5 time plate thickness) yielded defect free mechanically sound joint with improved (overmatched) tensile properties without compromising the impact toughness.
2. Sufficient plasticized material flow and grain refinement for proper coalescence of HSLA steel joint was achieved at the heat input of 1.05 kJ/mm and formation of lath upper bainitic stir zone microstructure could be the reason for high strength with acceptable impact toughness properties.

Acknowledgments The authors are grateful to The Director, Naval Material Research Laboratory (NMRL), Ambarnath for financial support through CARS project No: G8/15250/2011 dated 29.02.2012 and providing base material for this investigation. Also the authors are grateful to Dr. A. K. Lakshminarayanan, Associate Professor, SSN College of Engineering, Chennai, India for his valuable suggestions, guidance and discussion to carry out this investigation.

References

1. Fujii H, Cui L, Tsuji N, Maeda M, Nakata K, and Nogi K, *Mater Sci Engg A*, 429 (2006) 50.
2. Magudeeswaran G, Balasubramanian V, Reddy G M, and Balasubramanian T S, *J Iron Steel Res Int*, 15 (2008) 87.
3. Kang J, Wang C, and Wang G D, *Mater Sci Engg A*, 527 (2012) 96.
4. Lambert A, Drillet J, Gourgues A F, Stuel T, and Pineau A, *Sci Tech Weld Join*, 5 (2000) 173.
5. Lakshminarayanan A K, and Balasubramanian V, *Mater Des*, 31 (2010) 4600.
6. Thompson B, Babu S S, *Welding Research*, 89 (2010) 261.
7. Galvao I, Leal R M, and Loureiro A, *J Mater Process Technol*, 213 (2013)135.

8. Zhu X K, and Chao Y J, *J Mater Process Technol*, 146 (2004) 272.
9. Park S H C, Sato Y S, and Kokawa H, *Metal Mater Trans A*, 40 (2009) 636.
10. Gan W, Li Z T, and Khurana S, *Sci Technol Weld Join*, 12 (2007) 613.
11. Lienert T J, Stellwag J R, Grimmer B B, and Warke R W, *Weld Jour*, 89 (2003) 9.
12. Lakshminarayanan A K, and Balasubramanian V, *Metall Mater Inter*, 17 (2011) 981.
13. Malarvizhi S, and Balasubramanian V, *Mater Des*, 40 (2012) 460.
14. Ying-qiao Z, Han-qian Z, Jin-fu L I, and Wei-ming L I U, *J Iron Steel Res Inter*, 16 (2009) 80.
15. Rajamanickam N, Balusamy V, Magudeeswaran G, and Natara-jan K, *Mater Des*, 30 (2009) 2731.
16. Lee C H, Bhadeshia H K D H, and Lee H C. *Mater Sci Engg A*, 360 (2003) 249.
17. Wan X L, Wei R, and Wu KM, *Mater Charac*, 61 (2010) 731.
18. Brown I H, *Scrip Mater*, 54 (2006) 492.
19. Momeni A, Arabi H, Rezaei A, Badri H, and Abbasi S M, *Mater Sci Engg A*, 528 (2011) 2163.
20. Yamamoto K, Hasegawa T, and Takamura J. *ISIJ. Int*, 36 (1996) 86.
21. Ghosh K, and Mishra R S, *Scrip Mater*, 851 (2010) 85.
22. Dhua S K, and Sen S K, *Mater Sci Engg A*, 52 (2011) 6365.
23. Ghosh A, Das S, Chatterjee S, and Rao P R, *Mater Charac*, 56 (2006) 65.
24. Kenyon N, *Weld Jour*, 1968, 198.
25. Song K H, Fujii H, and Nakata K. *Mater Des*, 30 (2009) 3972.